

Supplementary Information

Solvent-free, self-emulsified and heat-responsive polyester coating enables chemically-recyclable and fire-safe PET foam

Bei-Bei Zhang, Li-Xia Fan, Lin Chen, Xiu-Li Wang, Yu-Zhong Wang**

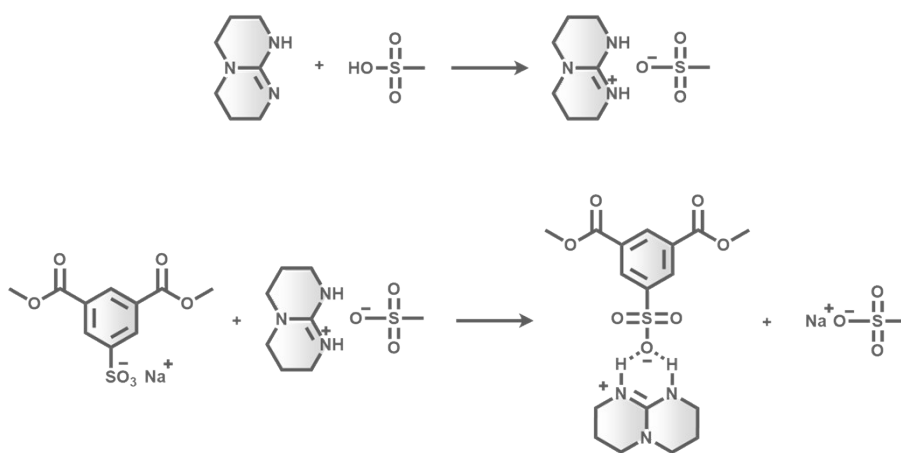
Collaborative Innovation Center for Eco-Friendly and Fire-Safety Polymeric Materials (MoE), National Engineering Laboratory of Eco-Friendly Polymeric Materials (Sichuan), State Key Laboratory of Polymer Materials Engineering, College of Chemistry, Sichuan University, Chengdu 610064, China

*E-mail: linchen410@scu.edu.cn; yzwang@scu.edu.cn

Experimental section

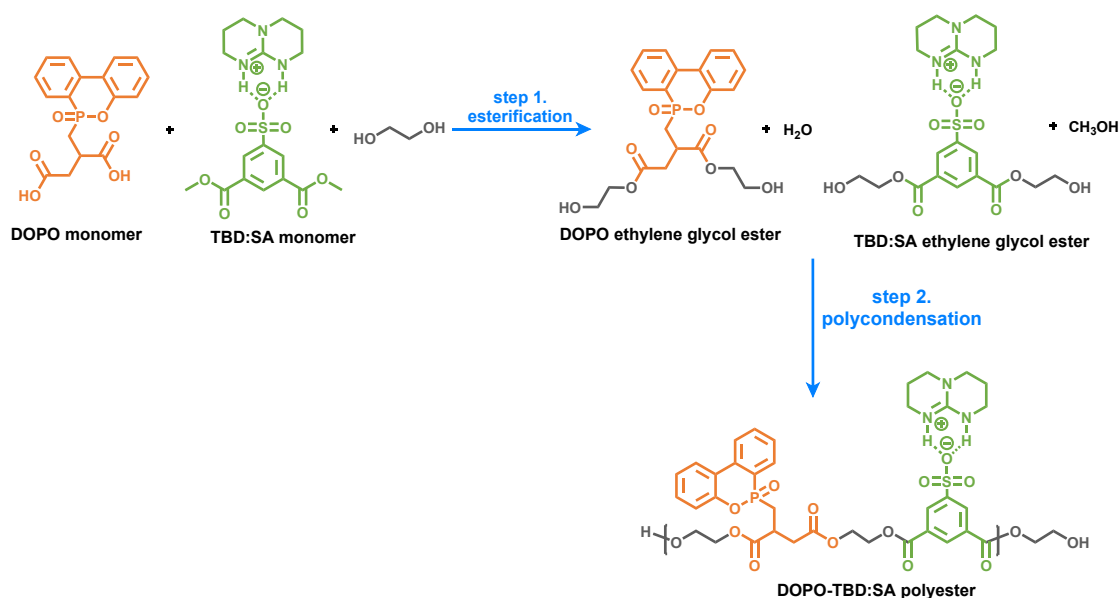
Materials: PET foam (PETF, density: 250 kg m^{-3}) was supplied by Yueke New Materials Co., Ltd. (Jiangsu, China). 1,5,7-triazabicyclo [4.4.0]-dec-5-ene (TBD) and methanesulfonic acid were supplied by Titan Scientific Co., Ltd. (Shanghai, China). Sodium dimethyl 5-sulphonatoisophthalate (SIPM), ethylene glycol (EG), tetrabutyl titanate (TBT), pyromellitic dianhydride (PMDA), dimethyl terephthalate (DMT) and methanol were supplied by Aladdin Biochemical Technology Co., Ltd. (Shanghai, China). 9,10-Dihydro-10-(2,3-dicarboxypropyl)-9-oxa-10-phosphaphenanthrene 10-oxide (DOPO monomer) and N, N-dimethylformamide (DMF) were supplied by Alfa Chemical Co., Ltd. (Zhengzhou, China). Deionized water was provided by the laboratory.

Synthesis of TBD:SA monomer. TBD:SA was synthesized by the two-step reaction as shown in **Scheme S1**. Firstly, a magneton, 6.96 g TBD and 50 mL deionized water were sequentially added into a 250 mL single-necked flask equipped with a condenser, and then 4.81 g methanesulfonic acid was added to react at $85 \text{ }^\circ\text{C}$ for 1 h. After the reaction, 14.91 g SIPM and 100 mL deionized water were added, and the mixture was stirred at $85 \text{ }^\circ\text{C}$ for 2 h. After the reaction, the product was cooled at room temperature for 12 h and filtered out. The product was purified by recrystallization from water and then dried in a vacuum oven. The yield of TBD:SA is 16.58 g, and the production rate is 80.3%.



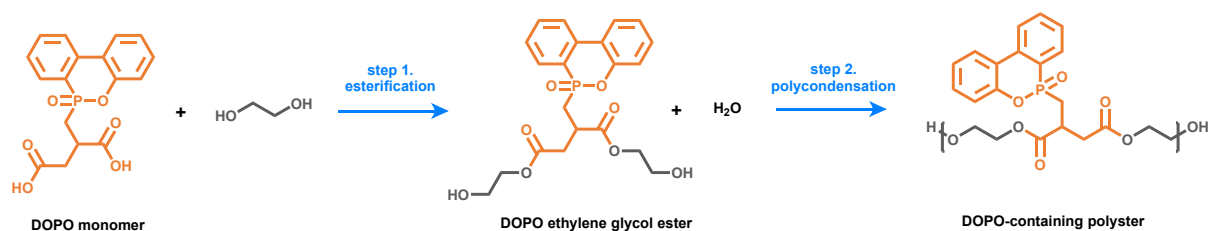
Scheme S1. Synthetic process of TBD:SA monomer

Synthesis of DOPO-TBD:SA polyester. DOPO-TBD:SA was synthesized by one-pot copolymerization of DOPO monomer, TBD:SA monomer and ethylene glycol as shown in **Scheme S2**. 93.00 g (1.5 mol) EG, 30.97 g (0.075 mol) TBD:SA, 25.95 g (0.075 mol) DOPO monomer and 75 μ L TBT were added into a 250 mL three-necked bottle with nitrogen protection and a mechanical stirrer. The mixture was mechanically stirred at 200 °C and normal pressure for 4 h to carry out esterification reaction. And then the polycondensation reaction was conducted at 200 °C for 3 h under a vacuum of 70 Pa. The yield of DOPO-TBD:SA polyester is 45.85 g, and the production rate is 78.0%. The loss of DOPO-TBD:SA polyester is mainly due to adhesion to the bottle wall.



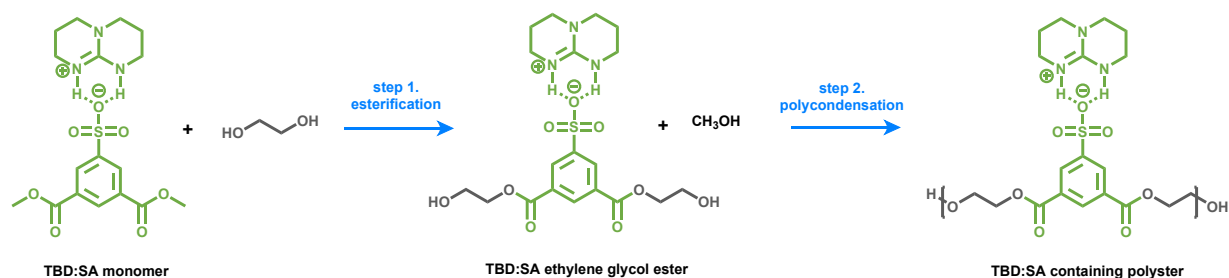
Scheme S2. One-pot synthetic routes of DOPO-TBD:SA polyester

Synthesis of only DOPO-containing polyester. As shown in **Scheme S3**, 46.50 g (0.75 mol) EG, 25.95 g (0.075 mol) DOPO monomer and 36 μ L TBT were added into a 250 mL three-necked bottle with nitrogen protection and a mechanical stirrer. The mixture was mechanically stirred at 200 °C and normal pressure for 4 h to carry out esterification reaction. And then the polycondensation reaction was conducted at 200 °C for 3 h under a vacuum of 70 Pa. The yield of DOPO-containing polyester is 22.60 g, and the production rate is 81.0%.



Scheme S3. One-pot synthetic routes of DOPO-containing polyester

Synthesis of only TBD:SA-containing polyester. As shown in **Scheme S4**, 46.50 g (0.75 mol) EG, 30.97 g (0.075 mol) TBD:SA and 39 μ L TBT were added into a 250 mL three-necked bottle with nitrogen protection and a mechanical stirrer. The mixture was mechanically stirred at 200 $^{\circ}$ C and normal pressure for 4 h to carry out esterification reaction. And then the polycondensation reaction was conducted at 200 $^{\circ}$ C for 3 h under a vacuum of 70 Pa. The yield of TBD:SA-containing polyester is 25.58 g, and the production rate is 82.9%.



Scheme S4. One-pot synthetic routes of TBD:SA-containing polyester

Preparation of polyester waterborne coating with different solid content. Without external emulsifiers, organic solvents and stirring, the 50~80% ultra-high solid contents waterborne coatings were formed by adding different mass ratio of DOPO-TBD:SA polyester and deionized water by standing still for 6 h.

Preparation of coated PET foam (PETF@DOPO-TBD:SA). The PETF@DOPO-TBD:SA (coating mass of 25 mg cm^{-2}) was prepared with 80 wt% water dispersion by brush-coating and dried at 100 $^{\circ}$ C for 30 min.

Chemical recycling of PETF@DOPO-TBD:SA. 1.10 g PETF@DOPO-TBD:SA (coating mass of 25 mg cm^{-2}) was cut into little pieces. And then the PETF@DOPO-TBD:SA

pieces, 22.00 g methanol and a magneton were putted into a SLM50 hydrothermal reactor (Sen Long, Beijing) and stirred at 160 °C for 20 h. After cooling for 12 h, white needle-like crystals precipitated from methanol and were filtered to obtain the recycled PET monomer (marked as DMT-1). The separated liquid was distilled under reduced pressure to remove most of the methanol, and 100 mL of deionized water was added to precipitate some white solid (marked as DMT-2). The white solid DMT-2 and the liquid were separated by filtration. The remaining liquid was distilled under reduced pressure to remove water, thereby obtaining a mixture of DOPO-monomer, TBD:SA monomer and ethylene glycol. The sum of the dried DMT-1 and the dried DMT-2 was the weight of the recycled DMT. The recycled rate of DMT (R_{DMT}) is calculated using the following equation (1),

$$R_{DMT} = \frac{m_{DMT}}{194 \times \frac{m_{PET}}{192}} \quad (1)$$

where m_{DMT} and m_{PET} are the weight of the recycled DMT and weight of PET in PETF@DOPO-TBD:SA, respectively. The molecular weights of the DMT and PET repeat unit are 194 g mol⁻¹ and 192 g mol⁻¹, respectively.

Characterization

Nuclear magnetic resonance (NMR) spectra was measured via a Bruker AVANCE AV II-400 NMR instrument at room temperature. TBD:SA monomer, DOPO-containing monomer, DOPO-containing polyester, TBD:SA-containing polyester, DOPO-TBD:SA polyester and recycled DMT were dissolved in deuterated dimethyl sulfoxide (DMSO-*d*₆). The mixture of recycled DOPO monomer, recycled TBD:SA monomer and recycled ethylene glycol were dissolved in a mixture of deuterated acetone and deuterated water (volume ratio is 1:1).

Thermogravimetric analysis (TGA) was performed by using a TG 209 F1 (NETZSCH, Germany) thermal analyzer model from 40 °C to 700 °C at a heating rate of 10 °C min⁻¹ under a nitrogen condition.

Differential scanning calorimetry (DSC) was performed by using a DSC2500 (TA, USA) from 40 °C to 260 °C at a heating rate of 10 °C min⁻¹ under a nitrogen flow with a rate of 50

mL min⁻¹.

The particle size was determined by dynamic light scattering (DLS) by using a Malvern ZEN3690 at 25 °C. The dispersion was diluted in deionized water to 1 g L⁻¹ to avoid the effects of multiple scattering in DLS testing.

The zeta potential was determined by electrophoretic light scattering (ELS) by using a Malvern ZEN3690 at 25 °C.

The weight-average molecular weight (M_w) was determined by static light scattering (SLS) by using a Malvern ZEN3690 at 25 °C. A glass cuvette was used for all SLS measurements. Toluene is as the standard sample. According to the Rayleigh expression, the average scattering intensities were related to polymer concentrations following equation (2),

$$\frac{KC}{R_\theta} = \left(\frac{1}{M_w} + 2B_2C\right) \frac{1}{P(\theta)} \quad (2)$$

$$\frac{KC}{R_\theta} = \frac{1}{M_w} + 2B_2C \quad (3)$$

$$K = \frac{2\Pi^2}{\lambda_0^4 N_A} \left(\tilde{n}_0 \frac{d\tilde{n}}{dC}\right)^2 \quad (4)$$

where in equation (2) K is an optical constant defined as equation (4), C is polymer concentration, R_θ is the Rayleigh ratio, M_w is the weight-average molecular weight, B_2 is the Second virial coefficient, P_θ is an angular dependence of the sample scattering intensity which approaches 1 when the polymer aggregations are smaller than the wavelength of the incident light. In this case, equation (2) can be transformed to equation (3). Where in equation (4) λ_0 is the incident light wavelength, N_A is the Avogadro's constant, \tilde{n}_0 is solvent refractive index,

$\frac{d\tilde{n}}{dC}$ is the differential refractive index increment. Single-angle static light scattering experiments were performed to determine the scattered light intensity of different sample

concentrations ($\frac{KC}{R_\theta}$), and obtain a graph called Debye-plot. M_w can be determined by the intercept at concentration of zero. B_2 can be determined by the slope of the plot.

The solid contents were measured according to GB/T 1725-1979 by drying a certain

amount of waterborne coating at 120 °C until the mass remaining constant, then calculating the weight ratio of residue to the whole waterborne coating.

The viscosities of waterborne coating with different solid content were measured by a rotary viscosimeter (NDJ-8S, Shanghai, China) at 25 °C.

The storage stability of dispersions was determined by putting them at room temperature for 3 months.

The interfacial adhesion strength of coating was measured using a universal testing machine (INSTRON 3366) at a rate of 2 mm min⁻¹. The size of single lap joint was 25 × 12.5 mm², and five samples were tested to get an average value. The compressive strength was also measured by a universal testing machine (INSTRON 3366) according to ASTM D1621-16 with a rate of 5 mm min⁻¹. The size of the sample was 50 × 50 × 50 mm³ and five specimens were tested to obtain an average value.

The UL-94 vertical burning was carried out by using a KB-RS apparatus according to ASTM D 3801-19 with a size of 127 × 13 × 10 mm³.

The limited oxygen index (LOI) values were determined by using an JF-6 oxygen index flammability gauge according to ASTM D 2863-17 with a size of 150 × 10 × 10 mm³.

The cone calorimetry tests were determined by using a FTT (UK) calorimeter according to ASTM E1354-17 with a size of 100 × 100 × 25 mm³.

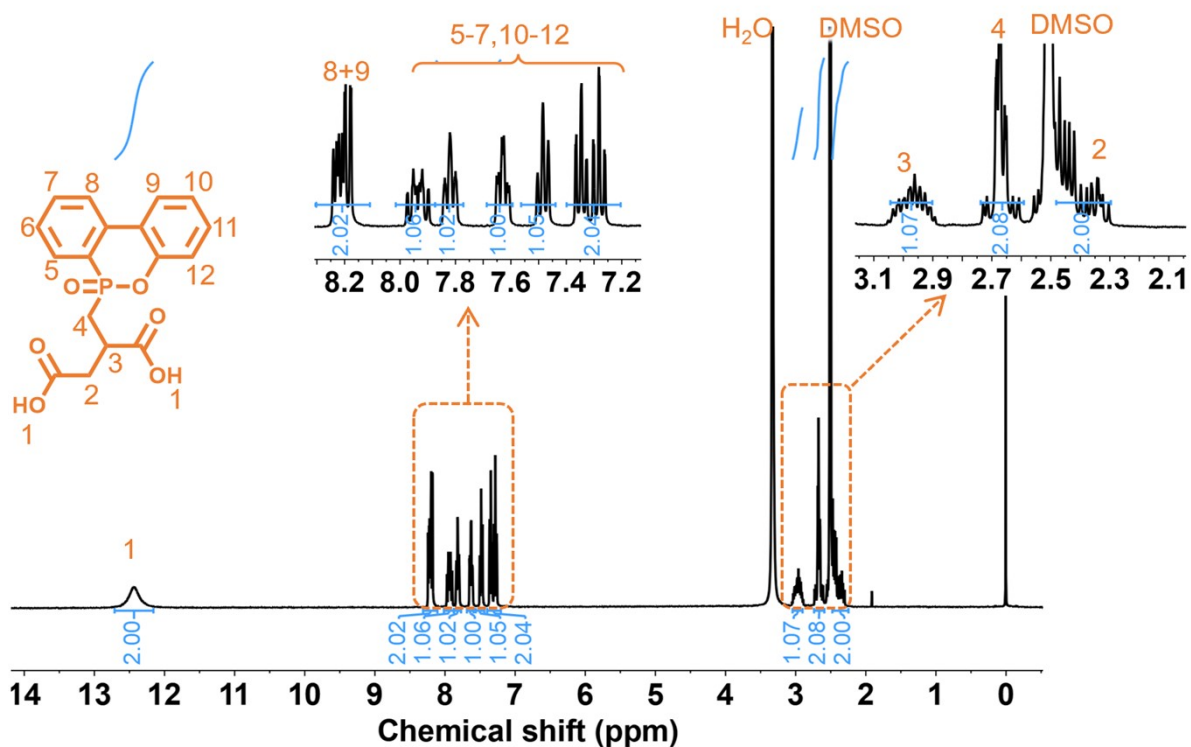


Fig. S1. ^1H NMR (400 MHz, $\text{DMSO-}d_6$, 25 $^\circ\text{C}$, TMS) of DOPO monomer with terminal carboxyl group

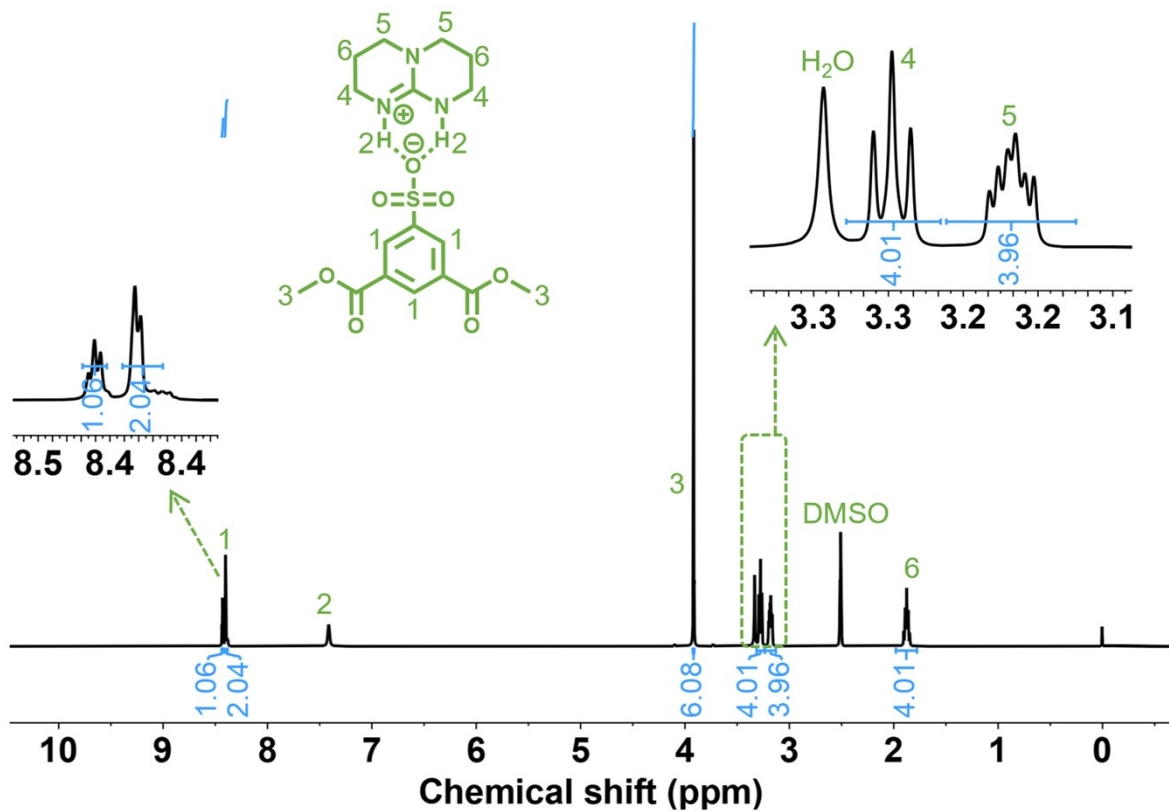


Fig. S2. ^1H NMR (400 MHz, $\text{DMSO-}d_6$, 25 °C, TMS) of TBD:SA monomer containing guanidine sulfonate (the integral area of active hydrogen in Peak 2 is insufficient).

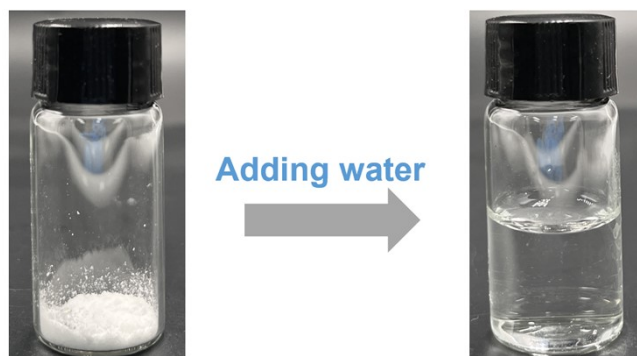


Fig. S3. Digital photos of TBD:SA monomer (left) and TBD:SA water solution (right)

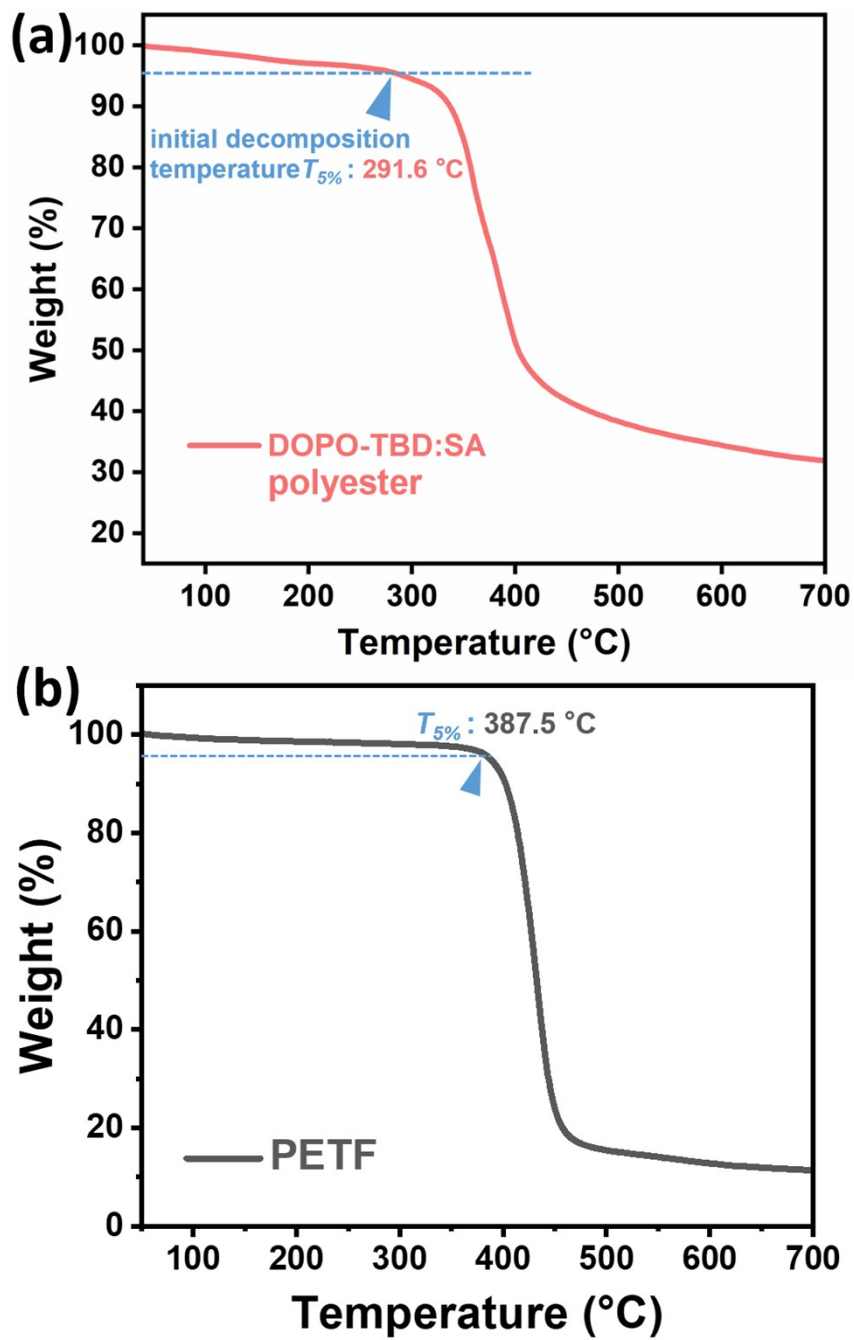


Fig. S4. Thermogravimetric curves of DOPO-TBD:SA polyester (a) and PET foam (b)

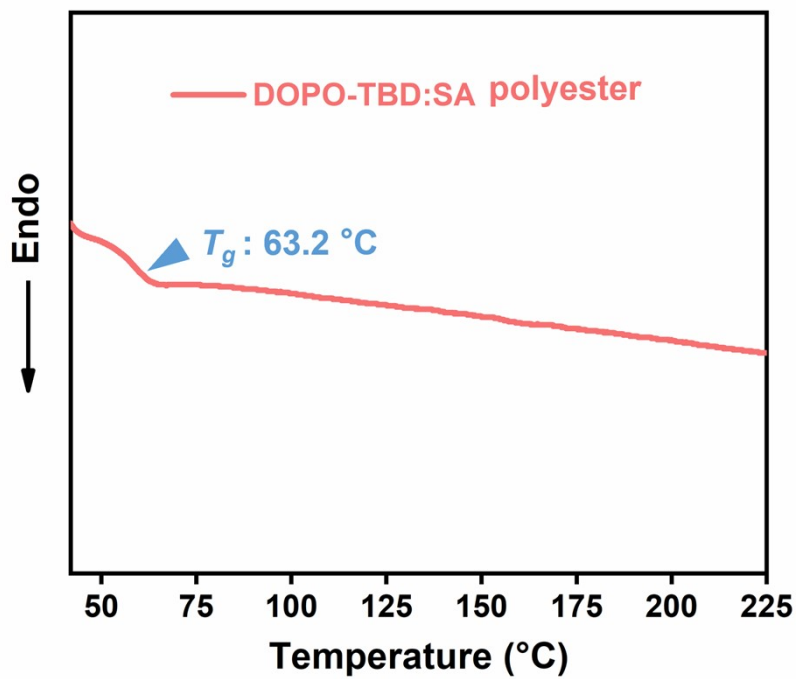


Fig. S5. DSC heating curve of DOPO-TBD:SA polyester

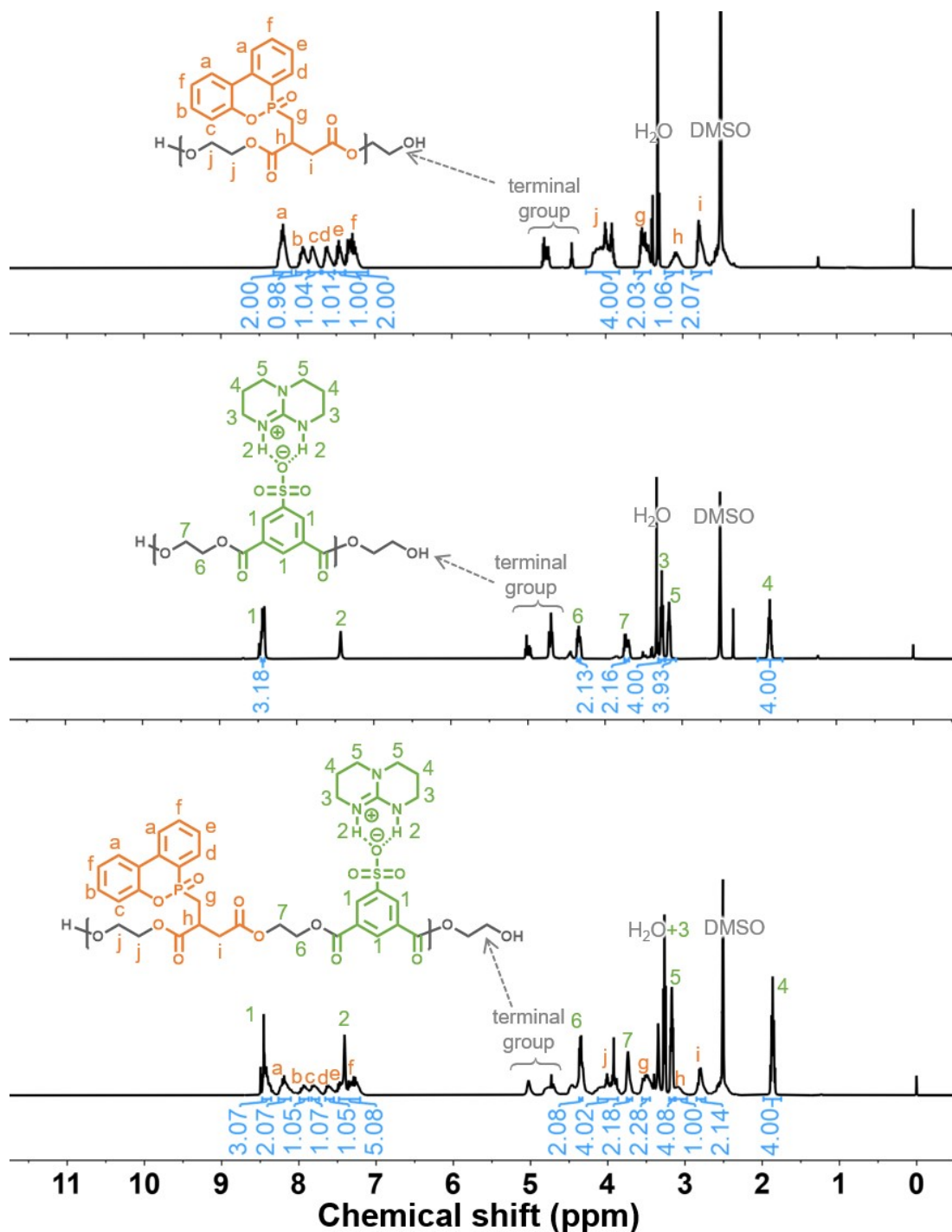


Fig. S6. ^1H NMR (400 MHz, $\text{DMSO-}d_6$, 25 $^\circ\text{C}$, TMS) of DOPO-containing polyester, TBD:SA-containing polyester and DOPO-TBD:SA polyester

To accurately attribute the chemical shifts of each hydrogen in DOPO-TBD:SA polyester, control polyester samples containing only DOPO monomer and only TBD:SA monomer are synthesized (Scheme S3-S4). The results show that each hydrogen in DOPO-TBD:SA polyester can be assigned, proving the successful synthesis of DOPO-TBD:SA polyester.

Table S1. Water dispersibility and flame retardance of polyester coating with different molar ratio of DOPO to TBD:SA

Molar ratio of DOPO to TBD:SA	Water dispersibility of coating	Flame retardance of PET foam with polyester coating
7:3	Poor	UL-94 V-0
6:4	Poor	UL-94 V-0
5:5	Good	UL-94 V-0
4:6	Good	UL-94 V-2
3:7	Good	UL-94 V-2



Fig. S7. Tyndall scattering effect of DOPO-TBD:SA polyester at 60%-80% high solid content in water

Table S2. Average particle diameter, polydispersity index and zeta potential of DOPO-TBD:SA dispersion in water (1 g L⁻¹).

Average particle diameter (nm)	Polydispersity index	Zeta potential (mV)
566	0.016	-80

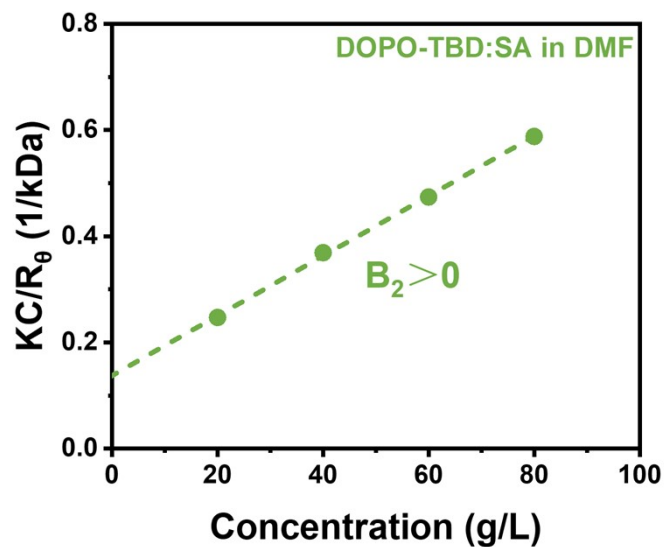


Fig. S8. Debye plot of DOPO-TBD:SA polyester in DMF

Table S3. Calculation data for DOPO-TBD:SA polyester in static light scattering test

solvent	Concentration (g/L)	$\frac{KC}{R_{\theta}}$ (1/kDa)	y-intercept	Molecular Weight (kDa)
water	0.25	1.55E-04	1.47E-04	6802.7
	0.5	1.73E-04		
	1	1.93E-04		
	1.5	2.12E-04		
DMF	20	0.247	0.1375	7.3
	40	0.369		
	60	0.474		
	80	0.588		

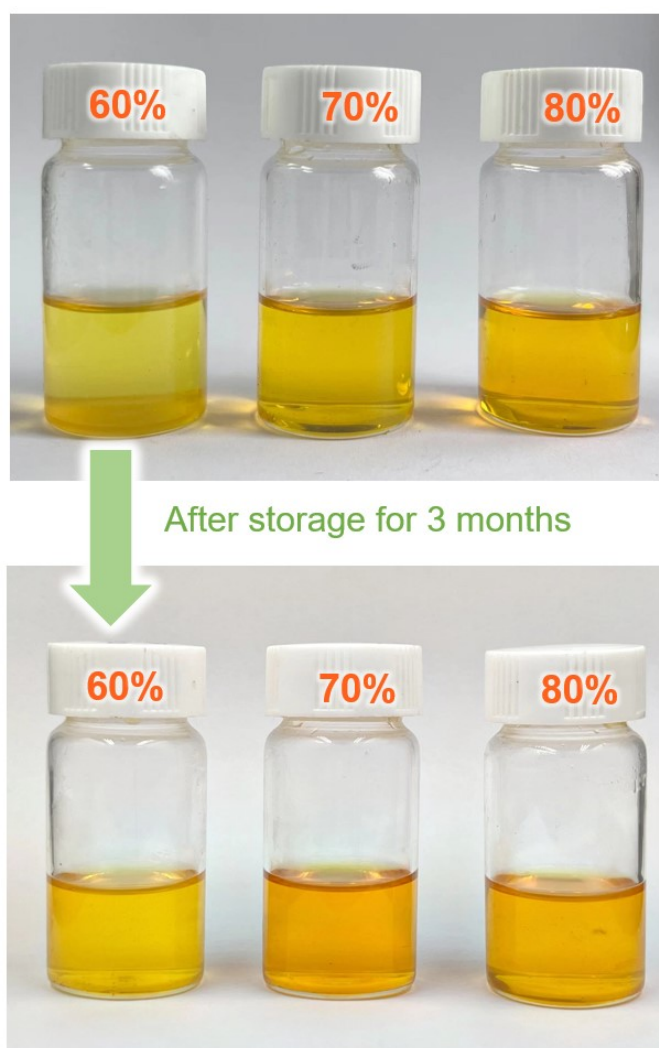


Fig. S9. Photos of DOPO-TBD:SA polyester coating after storage for 3 months

Table S4. Comparison of waterborne coating with high solid content in reported works

Polymer composition	Name	Organic solvent	Stirring	Solid content (wt%)	Viscosity (mPa·S)	Ref
Polyurethane resin	DCWPU	No	Rapid stirring	53.1 (max)	Not given	1
	SC-HWPU	Acetone	High-speed for 20 min	51.6 (max)	1291	2
	WPU-H	Acetone	600 rpm for 5 min	66.0 (max)	285	3
	FRWPU	Acetone	High-speed for 30 min	49 (max)	199	4
	Cationic WPU	Acetone	1500 rpm for 30 min	50.4 (max)	69	5
	WPU-Si8807	Acetone	High-speed for 1 h	59.9 (max)	2486	6
Acrylic resin	Poly (VeoVa-acrylate)	No	1200 to 2600 rpm	50	200-5000	7
	CNC-based formulations	No	High-speed	57.4	Not given	8
	MMA/BA/MAA	No	Surfactant, 220 rpm	60	Not given	9
	DMAPS/MMA/BA	No	200 rpm	50	Not given	10
	MTS/BA/MMA/AA	No	Emulsifier, 1000 rpm 30 min	54-57	147-398	11
	MMA/BA/MAA	No	Emulsifier, 350-1300 rpm	61-65	Not given	12
Alkyd resin	TESLOA	Acetone	Not given	40	gel	13
Epoxy resin	WPUME	Acetone	800 rpm 15 min	44.5	Not given	14
				50	91	
				60	123	
				70	225	This work
				75	1701	
Polyester	DOPO-TBD:SA	No	No	80	28397	

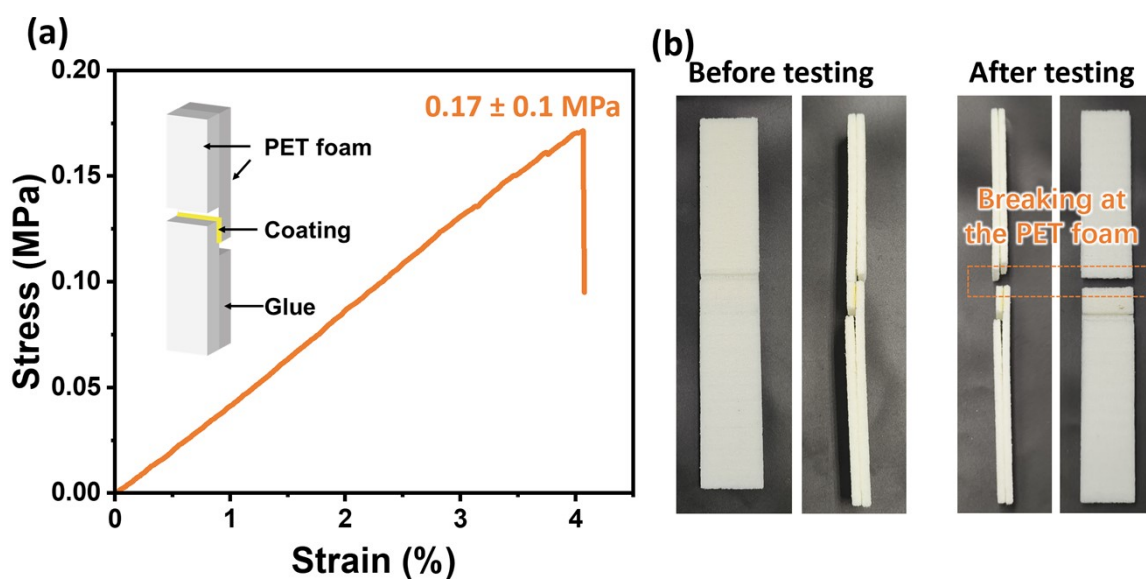


Fig. S10. (a) Tensile stress-strain curve of PET foam connected by DOPO-TBD:SA coating; (b) Digital photos of samples before and after testing.

The interfacial adhesion strength of DOPO-TBD:SA coating to the PET foam matrix is 0.17 ± 0.01 MPa. It is worth noting that the fracture site is the PET foam and not the coating (**Fig. S10b**), which means that the actual adhesion strength of the coating exceeds 0.17 MPa. This indicates that the coating has a relatively high interfacial adhesion to the PET foam.

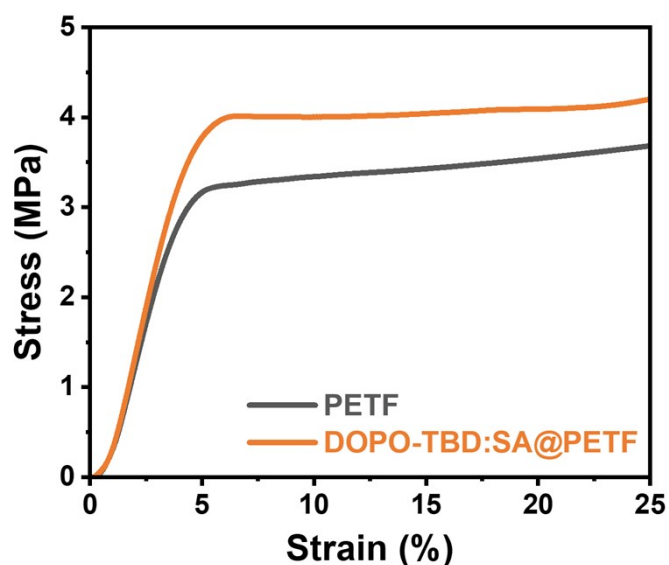


Fig. S11. Compressive stress-strain curves of PET foam and DOPO-TBD:SA@PETF foam

The coating-modified PET foam (DOPO-TBD:SA@PETF) exhibits higher compressive strength than PET foam, showing that the DOPO-TBD:SA coating has better compressive strength than the porous PET foam. These results indicate that the DOPO-TBD:SA coating maintains the original mechanical properties of PET foam.

Table S5. Classification standards for UL-94 flammability test

Test content	Rating		
	V-0	V-1	V-2
The flaming combustion time (s) of each specimen after each ignition is not more than	10	30	30
The flaming combustion time (s) of five specimens after 10 times of ignition is not more than	50	250	250
The flameless combustion time (s) of a specimen after the second ignition is not more than	30	60	60
Whether each specimen flame combustion or flameless combustion spread to the clamp.	No	No	No
Whether the dripping of each specimen ignite absorbent cotton	No	No	Yes

Table S6. Depolymerization rate of PETF and PETF@DOPO-TBD:SA under different reaction conditions

Sample	Temperature (°C)	Mass ratio of foam to methanol	Time (h)	depolymerization rate (%)
PETF	150	1:10	10	un-depolymerized
PETF@DOPO-TBD:SA	150	1:5	10	50
	150	1:10	10	65
	150	1:10	20	70
	150	1:20	20	77
	160	1:20	20	100

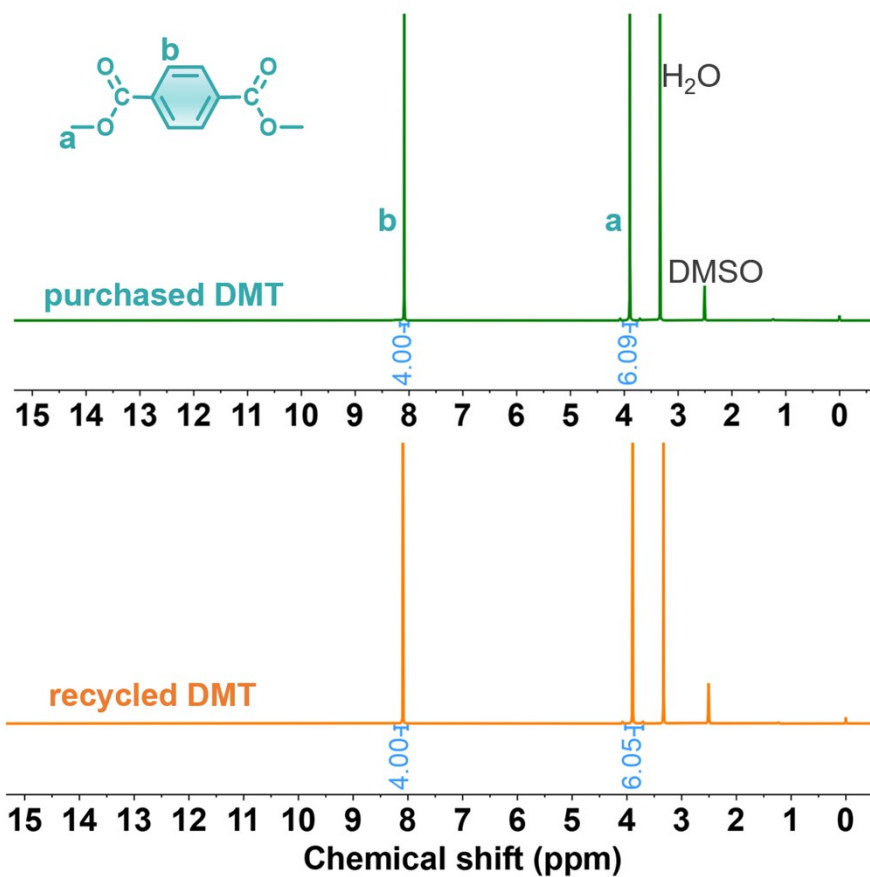


Fig. S12 ^1H NMR (400 MHz, $\text{DMSO-}d_6$, 25 $^\circ\text{C}$, TMS) of purchased DMT and recycled DMT

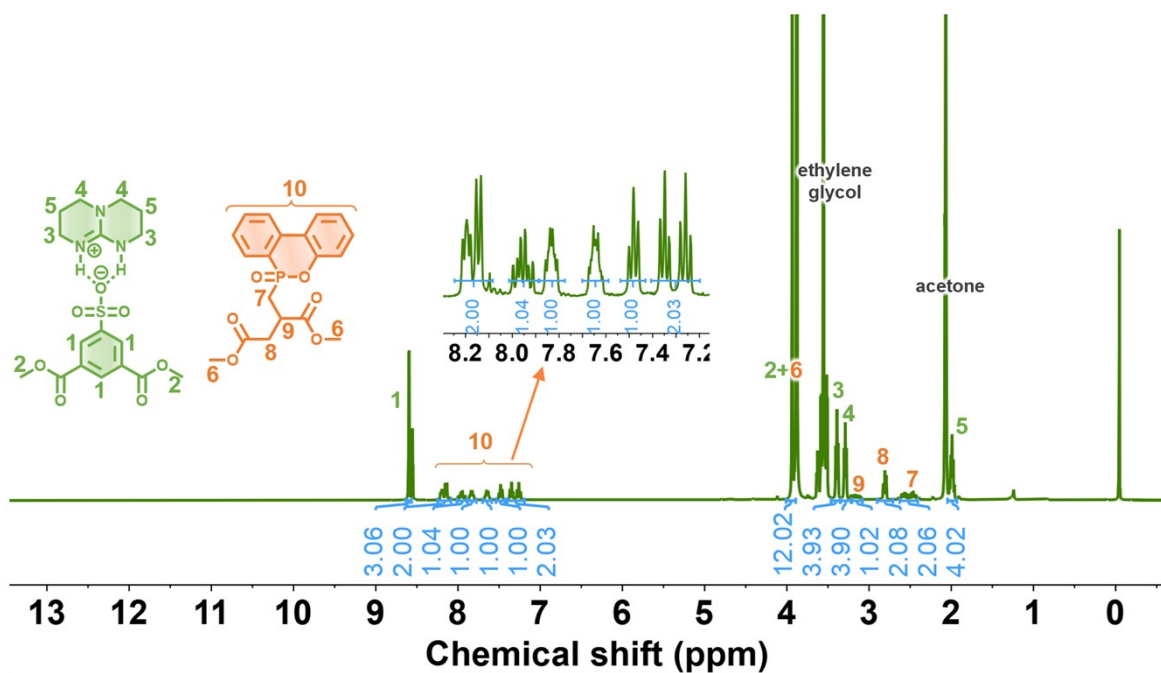


Fig. S13 ^1H NMR (400 MHz, mixed D_2O and $\text{acetone-}d_6$, 25 $^\circ\text{C}$, TMS) of the mixture containing recycled DOPO monomer, TBD:SA monomer and ethylene glycol

Reference

- [1] Zhang, Y., Zeng, R., Ban, T., Guo, M., Wang, Y., Zhang, J., Zhu, X. High Solid Content Waterborne Polyurethane and the Coatings with Double Crosslinking Structure and Multiple Hydrogen Bonds. *Colloids Surf. A Physicochem. Eng. Aspects.* **682**, 132816 (2024).
- [2] Qiao, P., Zhang, F., Lu, A., Liu, J., Jin, L., Wang, Y. Preparation and Characterization of High-Solid Carboxylate/Sulfonate Waterborne Polyurethane and Its Application in Novel Water-Based Superfine Fiber Synthetic Material. *J. Appl. Polym. Sci.* e55926 (2024).
- [3] Chai, C., Ma, Y., Li, G., Ge, Z., Ma, S., Luo, Y. The Preparation of High Solid Content Waterborne Polyurethane by Special Physical Blending. *Prog. Org. Coat.* **115**, 79–85 (2018).
- [4] Yin, Y., Feng, M., Li, W., Yao, J., Niu, J. Preparation and Performance Investigation of High Solid Content Flame Retardant Waterborne Polyurethane. *J. Appl. Polym. Sci.* **140**, e54674 (2023).
- [5] Mu, M., Liu, X., Bi, H., Wang, Z., Qian, C., Yao, B., Liu, Y., Liu, X., Li, X. Preparation and Characterization of High Solid Content Cationic Waterborne Polyurethane with Core-Shell Structures. *J. Appl. Polym. Sci.* **141**, e54766 (2024).
- [6] Diao, S., Zhang, Y., Zhao, C. *et al.* Preparation of waterborne polyurethane with high solid content: the crystallinity control of soft segment and the organosilicon modification. *Polym. Bull.* **81**, 317–333 (2024).
- [7] Abd El-Ghaffar, M. A., Sherif, M. H., Taher El-Habab, A. Novel High Solid Content Nano Siliconated Poly (Veova-Acrylate) Terpolymer Latex for High Performance Latex Paints. *Chem. Eng. J.* **301**, 285–298 (2016).
- [8] Kaboorani, A., Auclair, N., Riedl, B. *et al.* Cellulose nanocrystal (CNC)-based nanocomposites for UV curable high-solid coating systems. *J. Coat. Technol. Res.* **14**, 1137–1145 (2017).
- [9] Aguirreurreta, Z., de la Cal, J. C., Leiza, J. R. Preparation of High Solids Content Waterborne Acrylic Coatings Using Polymerizable Surfactants to Improve Water Sensitivity. *Prog. Org. Coat.* **112**, 200–209 (2017).
- [10] Murali, S., Agirre, A., Tomovska, R. Zwitterionic Monomers as Stabilizers for High Solids Content Polymer Colloids for High-Performance Coatings Applications. *Prog. Org. Coat.* **173**, 107196 (2022).
- [11] Neelambaram, P., Shankar, A., Sykam, K., Kumar, D. B. R., Chakrabarty, A., Narayan, R. Siloxane-Based High Solid Acrylic Latex by Mini-Emulsion Polymerization for Coatings with Improved Water Resistance. *Prog. Org. Coat.* **171**, 107011 (2022).
- [12] Mariz, I. de F. A., Millichamp, I. S., de la Cal, J. C., Leiza, J. R. High Performance Water-Borne Paints with High Volume Solids Based on Bimodal Latexes. *Prog. Org. Coat.* **68**, 225–233 (2010).
- [13] Salata, R. R., Pellegrene, B., Soucek, M. D. Synthesis and Properties of a High Solids Triethoxysilane-Modified Alkyd Coatings. *Prog. Org. Coat.* **133**, 340–349 (2019).

- [14] Zhang, J., Huang, H., Ma, J., Huang, L., Huang, L., Chen, X., Zeng, H., Ma, S. Preparation and Properties of Corrosion-Resistant Coatings From Waterborne Polyurethane Modified Epoxy Emulsion. *Front. Mater.* **6**, 185 (2019).